Macromolecular Materials and Engineering
Open Access
www.mame-journal.de

Tribological Performance of Bamboo Fabric Reinforced Epoxy Composites

Bernardo Antonio Oliver, Qiao Dong, Maziar Ramezani, Miguel Angel Selles, and Samuel Sanchez-Caballero*

Bamboo fiber is one of the strongest natural fibers with high strength-to-weight and stiffness-to-weight ratios and can be used economically for manufacturing fiber-reinforced composites. In this paper, bamboo fabric-reinforced epoxy composite is manufactured and its tribological properties for load-bearing applications are investigated. Sliding wear tests are conducted using a linear reciprocating tribometer and the effect of dry and lubricated contact conditions, applied load, sliding speed, temperature, and woven fabric direction on the coefficient of friction and wear rate are investigated. A scanning electron microscope is used to define the wear mechanisms at room and elevated temperatures. It is observed that the fabric orientation influences the mechanical and tribological performances of the composite material. Wear rate increases at higher loads and working temperatures; however, the effect of sliding speed is not remarkable, especially under lubricated contact conditions. The results present in this paper can be used for designing bamboo-reinforced epoxy composites for load-bearing applications, under different working conditions.

1. Introduction

Composite materials play an important role in different industries due to their unique mechanical, physical, and morphological properties.[1–4] Fiber-reinforced composite materials provide high strength-to-weight and stiffness-to-weight ratios, high toughness, good fatigue properties, and corrosion resistance.[5,6] They can also be used as load-bearing parts, for instance as orthopedic implants, where wear resistance and load-carrying capacity are important design parameters.[7]

To reinforce the composite materials, synthetic fibers such as carbon fiber, glass fiber and aramid fiber have been extensively used. However, with the trend to produce more environmentally friendly composite materials, natural fiber composites are emerging, and natural fibers such as bamboo, kenaf, banana, oil palm, sugarcane and coconut have been investigated by scientists and technologists around the world.[8–11]

Among these previous works, the study conducted by Chin et al.[12] investigated the utilization of kenaf fibers as a reinforcement material for tribo-composites based on epoxy for bearing applications. The study found that the presence of kenaf fibers in the composite material improved the wear and frictional performance of the epoxy. Additionally, Pothan et al.[13] examined the impact of fiber surface treatments on the interaction between the fibers and matrix in banana fiber-reinforced polyester composites. The study revealed that chemical modification had a profound effect on the fiber–matrix interaction, and a simple alkali treatment with NaOH at a concentration of 1% was the most effective. Moreover, Maleque et al.[14] studied the tensile, flexural, and impact properties of pseudostem banana fiber-reinforced epoxy composites. Jacob et al.[15] also investigated the effects of fiber length and concentration on the mechanical properties of natural rubber composites reinforced with sisal/oil palm hybrid fibers and found that increasing the fiber length or concentration resulted in a decrease in the material properties.

In another study, Yousif et al.[16] examined the effect of oil palm fibers on the tribological performance of polyester composites. The study discovered that the presence of oil palm fiber in the polyester improved the wear properties. El Tayeb[17] explored the tribological potential of sugarcane fiber reinforcement in thermoset polymers and found that sugarcane fiber/polyester composites show promise as tribo-materials. Finally, Nirmal et al.[18] investigated the wear and frictional characteristics of the treated betelnut fiber reinforced polyester (T-BFRP) composite and found that the wear and frictional performance of the composite improved under wet contact conditions.

Natural fibers have several advantages over synthetic fibers, including low density, low cost, high aspect ratio, good specific

B. A. Oliver, M. A. Selles, S. Sanchez-Caballero
Department of Materials and Mechanical Engineering
Universitat Politècnica de València
Alcoy 03801, Spain
E-mail: maselles@dimm.upv.es
Q. Dong, M. Ramezani
Department of Mechanical Engineering
Auckland University of Technology
Auckland 1010, New Zealand

The ORCID identification number(s) for the author(s) of this article can be found under https://doi.org/10.1002/mame.202300077

DOI: 10.1002/mame.202300077

properties, as well as abundant availability and being biodegradable and renewable.[8] Among the natural fibers, bamboo has attracted significant attention, because of its unique properties, including high stiffness and strength.[19,20] Bamboo can be harvested in three to four years after plantation and is a sustainable source of environmentally friendly biodegradable natural fiber with acceptable mechanical properties for fiber-reinforced composite materials, especially for structural and load-bearing applications.[21–24]

Bamboo is one of the fastest-growing plants, with a growth rate of up to 100 cm per day.[25] This material reveals a pronounced abundant fibril structure, which is easily observed when a bamboo cane is broken. It is a herbaceous timber plant, which is present on virtually all continents, although there are two areas of greatest confluence, East/Southeast Asia and the Neotropics. According to some studies, bamboo grows naturally in ecosystems as a healing agent for ecosystem damage (fires, fallen trees), spreading rapidly over the free surface due to its ease of growth.[25]

There are several advantages of using bamboo fabric composites over bamboo fiber composites. Bamboo fabric composites are more durable than bamboo fiber composites due to the way they are constructed. Bamboo fabrics are made using bamboo leaves and wood shoots with solvents, whereas bamboo fiber composites are made by bonding bamboo fiber together with a binder or resin. The woven structure of bamboo fabric composites makes them stronger and more resistant to tearing, impact and wear.[3] Bamboo fabric composites are also more environmentally friendly than bamboo fiber-based composites because they use less energy and water during the production process. Bamboo fabric is made using hydrolytic alkalization and heterogeneous bleaching techniques. Additionally, bamboo fabric requires less water to produce than bamboo fiber, which makes it a more sustainable choice.[26] Finally, in terms of cost, bamboo fabric composites are generally less expensive to produce than bamboo fiber composites, making them more accessible and affordable to consumers.[27] These advantages make bamboo fabric composites a promising material for various engineering applications.

Epoxy resin is a thermoset commonly used as the matrix phase of fiber-reinforced polymer composites.[28] The epoxy resin shows excellent mechanical properties and chemical and corrosion resistance. However, due to its poor crack propagation resistance and low fracture toughness, it should be strengthened by fillers or fibers.[29] Several papers have already been published on the manufacturing and mechanical testing of natural fiber-reinforced epoxy composite, including bamboo fiber-reinforced epoxy.[30–36] Most of these studies focused on tailoring the composite material's mechanical properties; however, to use the bamboo fiber-reinforced epoxy composite in load-bearing applications, characterization of the tribological behavior of the composite is needed.

There are only a limited number of papers published on the tribological performance of bamboo-reinforced polymers, and none of them provides a comprehensive overview and characterization of the wear resistance of this composite material. James et al.[37] manufactured hybrid composites of varying stacking sequences made up of bamboo and jute fibers. Epoxy resin was used as the matrix and the tribological performance of the developed composite material was investigated by two-body abrasive wear tests. They reported the wear rates for different applied loads and sliding speeds; however, coefficient of friction (COF), lubrication, and wear mechanisms were not investigated.

Alajmi et al.[38] studied the wear resistance of bamboo fiber-reinforced epoxy composite using a block-on-ring set-up. They reported the friction coefficients and wear rates under six different loads but did not investigate the effect of sliding speed, working temperature or lubrication on wear resistance. Kumari and Kumar manufactured orthotic calipers using bamboo-reinforced epoxy composite and studied their tribological performance using a block on roller tribometer.[7] The COF and wear rate were reported for only a single loading condition, and no analyses were conducted on wear mechanisms or failure modes of the contact surface.

It can be observed that when it comes to the tribological characterization of the bamboo-reinforced epoxy polymers, there is a lack of systematic approach and comprehensive results that can be used for designing this composite material for load-bearing applications. Therefore, in this study, we focused on manufacturing bamboo fabric-reinforced epoxy composite material and conducted comprehensive tribological experiments to evaluate the composite material's wear resistance and wear mechanisms in dry and lubricated contact. The coefficient of friction and wear rates under different working conditions were obtained by linear reciprocating sliding wear tests, and scanning electron microscopy analyses were performed to define the wear mechanisms. The results presented in this paper will shed light on the performance of bamboo fabric-reinforced epoxy composites for load-bearing applications, where wear resistance, low friction, and load-carrying capacity are critical design parameters.

2. Experimental Section

2.1. Materials

The fabric used in this investigation was made of 100% bamboo fiber in a taffeta weave format supplied by BambroTex (Jiangsu, China). The fabric was made from the *Staphylococcus aureus* strain from uncontaminated regions of China. Bamboo fibers were obtained from raw materials of bamboo pulp. The production process involved refining bamboo pulp from bamboo through hydrolysis–alkalization and multi-phase bleaching. Thus, by employing the hydrolysis–alkalization process, it became possible to separate components such as lignin and xylans from bamboo fiber, which had a negative impact on the tensile strength of bamboo fibers, as previously demonstrated in the study by Shi et al.[39] Subsequently, the refined bamboo pulp was processed into bamboo fiber. The fibers obtained after this process were subsequently bundled, stretched and twisted by the ring-spun spinning process. Finally, the yarn obtained in this process was used to manufacture a bidirectional fabric, with a resulting grammage of 205 g m^{-2}, as seen in **Figure 1**. **Table 1** shows the physical properties of the bamboo fibers obtained, while **Table 2** shows those of the bamboo yarn. The variability in the breaking strength of the thread obtained from refined fiber in this study (13.42%) was significantly lower than that previously obtained by other authors with values between 21% and 22% when using unrefined bamboo fiber directly.[40,41] On the

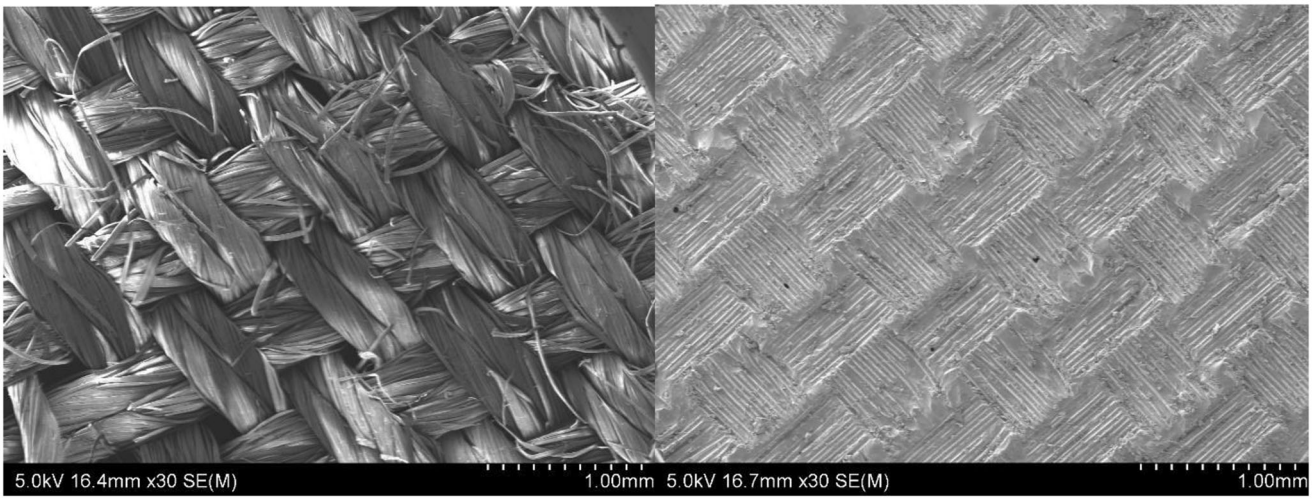

Figure 1. The surface of the woven bamboo fabric (left) and the composite material (right).

Table 1. Physical properties of bamboo fiber.

Property	Value	Units
Dry tensile strength	2.33	cN/dtex
Wet tensile strength	1.37	cN/dtex
Dry elongation at break	23.8	%
Linear density percentage of deviation	−1.8	%
Percentage of length deviation	−1.8	%
Overlength staple fiber	0.2	%
Overcut fiber	6.2	mg $100g^{-1}$
Residual sulphur	9.2	mg $100g^{-1}$
Defect	6.4	mg $100g^{-1}$
Oil-stained fiber	0	mg $100g^{-1}$
Coefficient of dry tenacity variation (CV)	13.42	%
Oil content	0.17	%
Moisture regain	13.03	%

Table 2. Physical properties of bamboo yarn.

Property	Value	Units
Yarn numbering	Ne40/1	-
CV	1.34	% Ne
Uster	11.39	U%
Thin	12	C50%
Thick	32	+50%
Neps	54	-
Hairiness	3.64	-
Elongation	12.5	%
CV	12.1	% Elongation
Tenacity	11.5	cN/tex
Humidity	11.72	%
Spinning system	Ring-spun	

other hand, the breaking strains of the thread used in this study (23.8%) were significantly higher than that of the thread from directly sourced bamboo fibers (0.88%), as reported in a previous study.[41] A Resoltech 1050 epoxy resin was used to manufacture the test specimens with varying materials to ensure a fair comparison between fabrics. This resin, supplied and packaged by *Resinas Castro*, Spain, was formulated to cure at room temperature without needing post-curing. To activate the curing process, the resin was mixed with a catalyzing agent in a mass ratio of 100:35 (resin: catalyst). Depending on the hardener chosen, gelification times varied from 10 min to 14 h allowed a wide range of applications.

The hardener chosen was 1056S, which provides 58 min. of gelification time for a thickness of 40 mm. and 235 min. for a thickness of 2 mm. The 1050 resin has a density of 1.14 kg m^{-3}, while that of the 1056S catalyst is 1.10 kg m^{-3}. This resin was chosen to manufacture the laminates because it offers good mechanical properties, excellent fatigue resistance and, above all, excellent properties for impregnation of the reinforcements.[42] The data sheet defines a maximum tensile strength of 97 MPa, an elastic modulus of 3.35 GPa, an elongation of 5% and a hardness of 86 Shore D, all after 14 days.

2.2. Manufacturing Process

To manufacture the specimens, the first step was to prepare the different samples of fabrics to be infused, to create the plates, and to group all the materials and tooling to be used. The process began by unrolling the fabrics and marking the cutting lines, using a straight steel profile as a guide to form the rectangular areas of the plate. Then, the fabrics were cut using specific scissors for cutting industrial technical fabrics. The resin infusion process started once the mold was cleaned with solvent and the bamboo fabrics were positioned side by side with different orientations. This way, obtaining plates of different orientations in a single infusion was possible.

The next step was to place on the material a peelable fabric of a larger size, ≈10 mm. perimeter offset. Then the diffusion mesh, of the same size as the peel ply, was positioned over the peel ply.

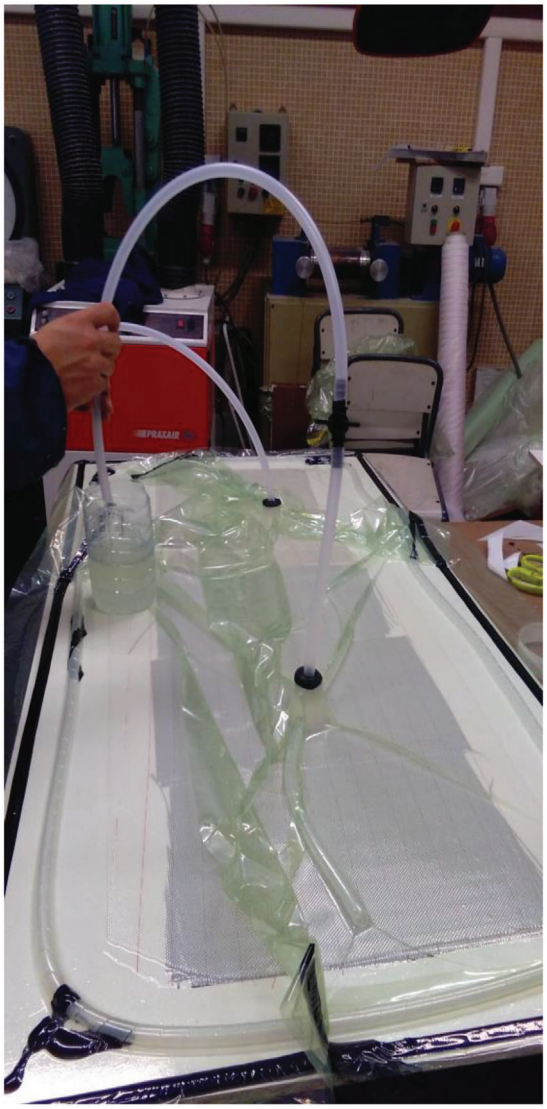

Figure 2. The manufacturing process of composite specimens.

In the center of the diffusion mesh, two infusion sockets were positioned with a length of helical tubing in each one to facilitate the entry of the resin into the set. The helical tube was then installed to absorb the resin from the sides, surrounding the perimeter of the mesh and outside it the sealing putty. The helicoidal tubes were coupled with the vacuum ducts of the pump using an LDPE T-type union, leaving them above the diffusion mesh to facilitate air extraction and fixing them with a small piece of adhesive tape. Once everything was in place, it was covered with a vacuum bag and the extraction ports connected to the pump.

The 1050 epoxy resin with the 1056S catalyst used in the process had a gelification time of 58 min., meaning that the manufacturing process must be completed within this timeframe before the resin polymerization began. To obtain good results, the manufacturer's specifications described in the product data sheet, were to use 35% catalyst by mass.

Once the infusion process was completed (**Figure 2**), the plates were left to cure for one day. Subsequently, they were demolded and the excess material was cut off. Once the manufacturing process of the plates was completed, they were cut using a circular saw and the final cut of the specimen geometry using a Computer Numerical Control (CNC) milling machine. The plates had a percentage of 48.81% of resin and 51.19% of fiber, with a grammage of 2.404 kg m^{-2} and a density of 1.265 kg m^{-3}, with 6 layers of taffeta bamboo fabric (**Table 3**).

Table 3. Characteristics of the resin, and composite materials.

Characteristics	
Resin	Resoltech 1050 epoxy, Density of 1.14 kg m^{-3}, Maximum tensile strength of 97 MPa, Elastic modulus of 3.35 GPa, Elongation of 5%.
Composite	48.81% of resin and 51.19% of fiber, with a grammage of 2.404 kg m^{-2} and a density of 1.265 kg m^{-3}, with 6 layers of fabric.

2.3. Tensile Tests

Before testing, the physical and geometrical properties of the specimens were recorded. It was necessary to measure the width and thickness of each sample with a caliper the width and thickness of each sample to calculate its effective stress area. The dimensions of the tested specimens, expressed in millimeters, are shown in **Figure 3**. Tests were conducted using a universal testing machine (IBERTEST, model ELIB-50, Madrid, Spain).

The test procedure included positioning the specimen between the grips and applying a pre-stress. Then the test was started, and the upper jaw began to move to generate a gradual deformation by increasing the distance between the jaws, and consequently stress in the axial direction. The software recorded the force and displacement values to plot the stress–strain graphs based on ISO 527-1 standard. Tensile tests were conducted on fifteen specimens, five cut with fiber orientation at 0, five cut at 90°, and the other five cut at 45°.

2.4. Compression Tests

The compression test measured the resistance of a specimen against a negative axial force intended to compress the material. From this test, it was possible to obtain the unit stress–strain diagram. Before the compression tests, the specimen dimensions were measured and were done with the IBER-TEST testing machine, model ELIB-50. Compression tests were carried out on four parallelepiped-shaped specimens with a width of 42 mm, a length of 13 mm, and a thickness of 6 mm.

The test consisted of subjecting the specimen to a gradual deformation by decreasing the separation between the two plates of the test fixture. The plate guiding system restricted the movement in two axes and allowed only the displacement in the central axis, so only axial compressive stress was exerted on the specimen. Each test was terminated when the force dropped on the specimen occurred.

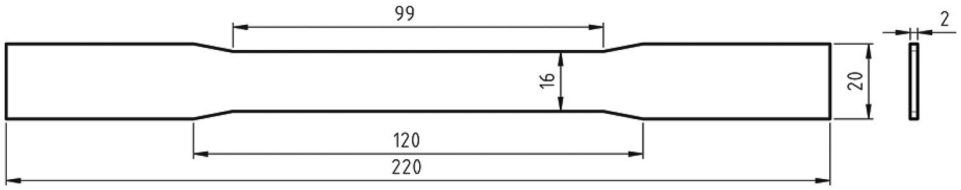

Figure 3. Tensile specimen dimensions in mm.

Table 4. Sliding wear conditions.

Load	20 N, 30 N, 40 N
Frequency	2, 5, and 8Hz
Temperature	23, 50, 100, and 150
Contact condition	Dry – lubricated with gear oil
Sliding stroke	10 mm
Sliding distance (cycle)	500 m (thus 50 000 cycles)

2.5. Sliding Wear Tests

A linear reciprocating tribometer (Ducom Instruments TR-282) was used to conduct the sliding wear experiments. The bamboo fabric composite samples were 40 mm × 20 mm × 5 mm and were cut in three different directions: 0°, 45°, and 90°. A range of normally applied loads, sliding frequencies and temperatures were used for the sliding wear tests, as listed in **Table 4**. The experiments were conducted in dry and lubricated conditions with a 10 mm diameter tungsten carbide ball as the counter material and gear oil used as a lubricant. The tribometer was set for a wear track (sliding stroke) of 10 mm, and a total sliding distance of 500 m was used for all tests. Before the sliding wear tests, all samples were kept in a controlled laboratory environment with a constant temperature of 23 °C and a relative humidity of 55%. Each test set was repeated at least three times, and the average values of the COF and wear rates were reported in this paper.

A stylus profilometer (Taylor Hobson Form Talysurf 50) was used to measure the cross-sectional area of the wear tracks. The profilometer scanned five sections of each wear track to obtain a raw profile graph of the worn surface of the sample, which determined the depth and width of the wear scars. Image analysis software, Image J, was used to calculate the average wear scar surfaces. The average cross-sectional area was multiplied by the wear track length (10 mm) to obtain the wear volume. Wear rates were then calculated using Equation (1).

$$\textit{Specific wear rate}\left(\frac{mm^3}{N.m}\right) = \frac{\textit{Average Wear Volume}\left(mm^3\right)}{\textit{Applied Load}\ (N) \times \textit{Wear Distance}\ (m)} \quad (1)$$

To observe the wear mechanisms, the tested samples were examined under a scanning electron microscope (Hitachi SU-70 field emission SEM). The tested composite samples were not electrically conductive, so they were coated with platinum using a Hitachi E-1045 ion sputter coating machine.

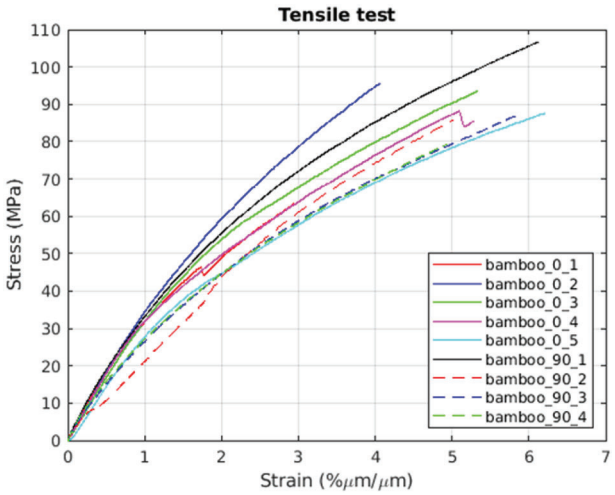

Figure 4. Tensile stress–strain diagram for 0° and 90° bamboo specimens.

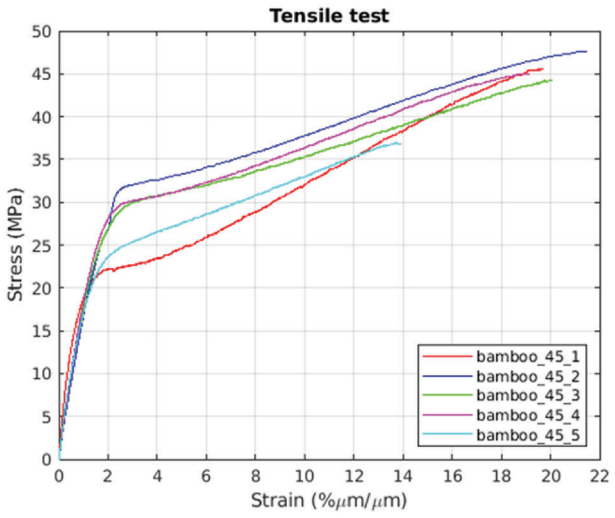

Figure 5. Tensile stress–strain diagram for ±45° bamboo specimens.

3. Results and Discussion

From the tensile tests, it has been possible to generate the stress–strain graph, as shown in **Figures 4** and **5**. The stress-elongation maximum values for 90° and ±45° tensile tests can be obtained from **Table 5**. Figure 4 shows how all 6 experiments provided similar results, one of them reaching 104 MPa of maximum stress. If we compare the results of the 90° and 45° orientations, the parts with 90° orientations are stronger but suffer a lower elongation.

Table 5. Stress-elongation maximum values for 90° and ±45° tensile tests.

Bamboo fiber orientation	Max stress [MPa]	Bamboo fiber orientation [%]
90°	107	6.2
±45°	47	21.8

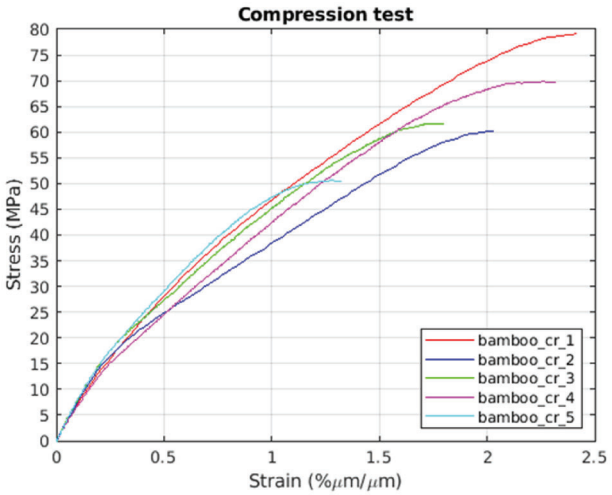

Figure 6. Compression stress–strain diagram for 90° bamboo specimens.

Figure 5 shows a slope change, showing an irreversible plastic deformation due to the alignment of the fibers when breaking part of the matrix.

Figure 6 shows the compression test results. The stress-elongation maximum values for 90° compression tests can be seen in **Table 6**. These values are lower than those of the tensile tests. This difference can be attributed to the distinct failure mechanisms that occur in each test. In compression tests, bamboo fibers are susceptible to a type of failure known as kinking. Kinking occurs when the fibers buckle and crack along an axis perpendicular to the fiber's orientation. This process results in the fibers breaking under compressive stress, ultimately reducing the material's overall strength and load-bearing capacity in compression tests. Conversely, tensile tests subject the fibers to tensile stress, causing them to elongate and eventually rupture when the stress reaches the material's tensile strength. This distinct failure mode allows the fibers to withstand higher stress values before failing, resulting in greater stress-elongation maximum values compared to compression tests.

Figure 1 shows the scanning electron microscope (SEM) images of the woven bamboo fabric and the composite materials, offering a detailed look into their microstructural characteristics. The images reveal that the bamboo fibers are woven in an organized and close-knit pattern, which contributes to the overall strength and durability of the fabric. The tight weaving of the fibers also enhances the material's resistance to wear. Furthermore, the SEM images provide insight into the interaction between the bamboo fibers and the epoxy matrix in the composite material. The epoxy matrix can be seen to encapsulate and protect the fibers effectively, ensuring that they are well-embedded within the composite structure. This coverage not only safeguards the fibers from environmental factors such as moisture and UV radiation but also helps in distributing the load evenly across the fibers, enhancing the composite's mechanical properties. Additionally, the epoxy matrix imparts a smooth and uniform surface to the composite material, which has numerous advantages. A uniform surface helps in reducing surface defects that could otherwise compromise the material's performance, such as stress concentrations or localized weak points.

Table 6. Stress-elongation maximum values for 90° compression tests.

Bamboo fiber orientation	Max stress [MPa]	Bamboo fiber orientation [%]
90°	79	2.4

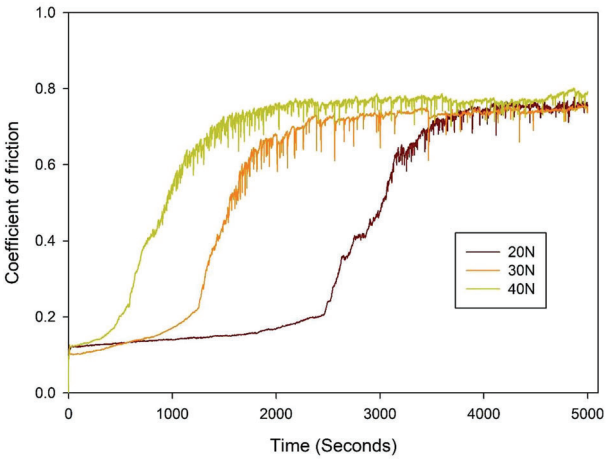

Figure 7. Coefficient of friction versus time at different normal loads, 5 Hz frequency at room temperature and under dry contact conditions tested in 45° direction.

Figure 7 shows the coefficient of friction versus time curves for 45° fiber direction bamboo composite samples tested under different normal loads. A low COF was observed at the beginning of the test for all samples. As the sliding wear test continues, the top resin layer wears out and the matrix is damaged. Therefore, the counter ball will be in direct sliding contact with the bamboo fibers, resulting in a significant increase in COF. It can be seen from Figure 6 that as the applied load increases, the time needed to remove the top resin layer decreases. However, as the contact between the counter ball and the bamboo fibers is established, the COF is almost the same value (≈0.8) under different applied normal loads. Similar behavior was observed in sliding wear tests of bamboo composite samples with 0° and 90° fiber directions.

As can be seen in **Figure 8**, a similar trend is observed for samples tested under different sliding speeds. As the frequency of the sliding motion increases, the time required to wear away the top epoxy matrix layer decreases, indicating that higher sliding speeds accelerate the wear process. As the top layer wears out and the tungsten carbide ball slides over the bamboo fabric, the COF increases significantly. This increase can be attributed to the higher frictional resistance of the bamboo fibers compared to the smooth epoxy matrix layer. Notably, after the tungsten carbide ball establishes direct contact with the bamboo fibers, the samples exhibit a consistent COF level. This suggests that the

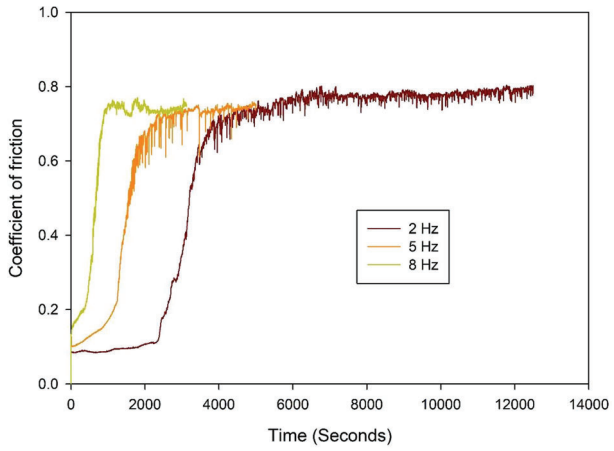

Figure 8. Coefficient of friction versus time at different frequencies, 30 N load at room temperature and under dry contact conditions tested in 45° direction.

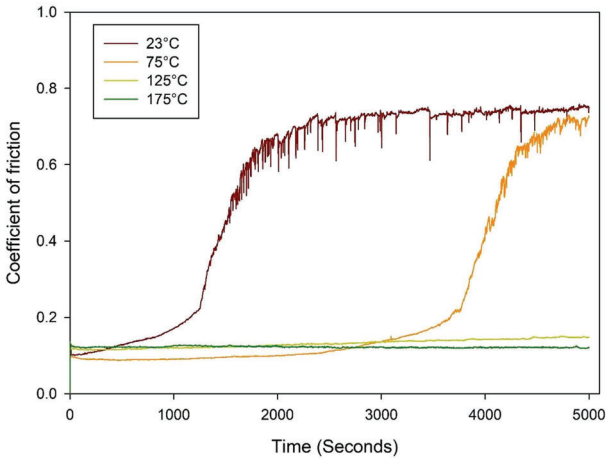

Figure 10. Coefficient of friction versus time at different temperatures, 30 N load, 5 Hz frequency tested in 45° direction.

frictional properties of the bamboo fibers remain relatively stable, irrespective of the sliding speed.

Figure 9 shows the SEM images of a sample wear track tested under 30 N load and 5 Hz frequency. As can be seen from the left image, the wear track has a 45° orientation from the bamboo fibers and the sample was tested under dry conditions. Examination of the SEM images highlights several important features of the wear track surface. Notably, micro-cracks can be observed perpendicular to the wear direction, indicating that the composite material experienced localized stress and damage during the wear test. Additionally, debris generated from the matrix wear appears to have been pressed into the surface, resulting in a relatively smooth wear track. This smoother surface may contribute to the material's overall wear resistance and frictional properties.

The primary wear mechanism observed in the SEM images is fatigue wear. Fatigue wear results from the repeated application of stress on the composite material during the wear test, leading to the formation of micro-cracks and eventual material removal. Localized surface deformations on the wear track also show that adhesive wear is another wear mechanism for this material. Importantly, these wear mechanisms and tribological properties were found to be consistent across samples with wear tracks oriented at 0° and 90° relative to the bamboo fibers. This consistency suggests that the bamboo composite material exhibits similar wear behavior and resistance to wear-related damage, irrespective of the orientation of the fibers relative to the wear track. This robustness further supports the potential suitability of bamboo composites for applications requiring wear resistance and low friction.

The samples were also tested at different temperatures (up to 175 °C) and the results are presented in **Figure 10**. The time needed to remove the top resin layer increases as the temperature increases. At temperatures above 100 °C, the epoxy resin matrix undergoes a softening process, which alters its mechanical properties and interaction with the embedded bamboo fibers. The softened resin tends to blend more effectively with the fibers, resulting in a more cohesive and resilient protective layer.

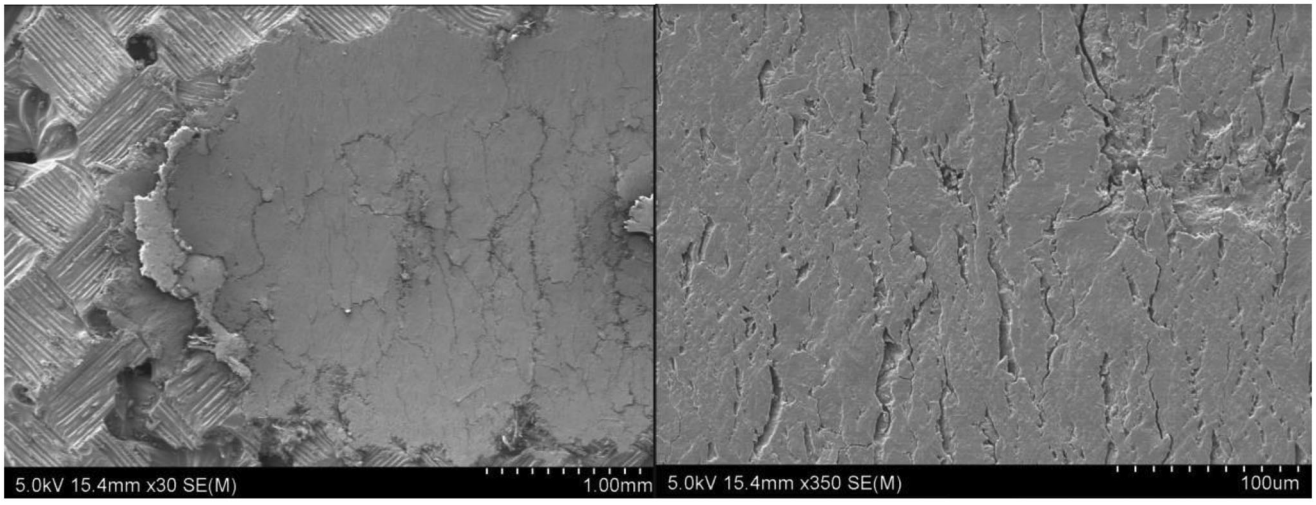

Figure 9. Wear track of the specimen tested under 30 N load, 5 Hz frequency at room temperature, dry contact condition and in 45° direction.

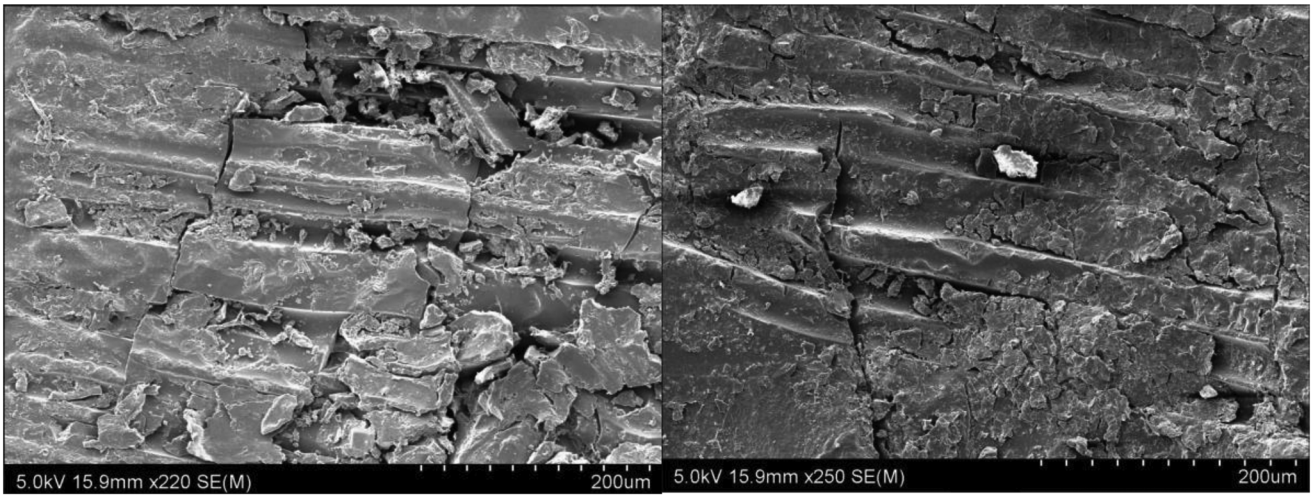

Figure 11. Wear track of the specimen tested at different temperatures (125 °C left, 175 °C right), under 30 N load, 5 Hz frequency and in 90° direction.

Consequently, this protective layer remains intact throughout the duration of the wear test, even under the influence of sliding contact with the counterface. The friction coefficient observed during the wear tests conducted at temperatures above 100 °C is remarkably low, registering values close to 0.1. The low COF indicates that this composite material is a great choice for load-bearing applications at elevated temperatures.

Figure 11 shows the SEM images of the wear tracks at higher temperatures (125 and 175 °C). The presence of wear debris and micro-cracks on the wear track surface indicates abrasion wear and fatigue wear occurring during the sliding tests. Wear debris results from the material removal process, where the harder counterface slides against the composite surface, while microcracks form due to the repeated stress and strain experienced by the material during the wear process. Additionally, the SEM images show spalling in certain regions of the wear track surface, which suggests that adhesive wear is another wear mechanism present in the composite material at higher temperatures. Spalling is characterized by the detachment or flaking of material fragments from the surface, often due to the strong adhesive forces between the contacting surfaces during sliding. The material transfer and subsequent bonding can result in the formation of local stress concentrations, which can lead to material removal as the contact continues. The observation of these wear mechanisms (abrasion, fatigue, and adhesive wear) at elevated temperatures highlights the complex material behavior and tribological properties of the bamboo composite.

The effect of lubrication on the wear resistance of the composite material was also investigated by running sliding wear tests with gear oil. **Figure 12** shows the impact of lubricated contact on COF at different applied loads. It can be seen that under gear oil lubrication, COF is low (between 0.08 and 0.12). As the normal load increases, the COF increases due to the formation of a thinner lubricant film at higher applied loads. The results showed that gear oil lubrication effectively reduces friction in the bamboo-reinforced composite material. The effect of sliding speed on COF in the lubricated condition is also shown in **Figure 13**. It can be observed that at higher sliding speeds, COF

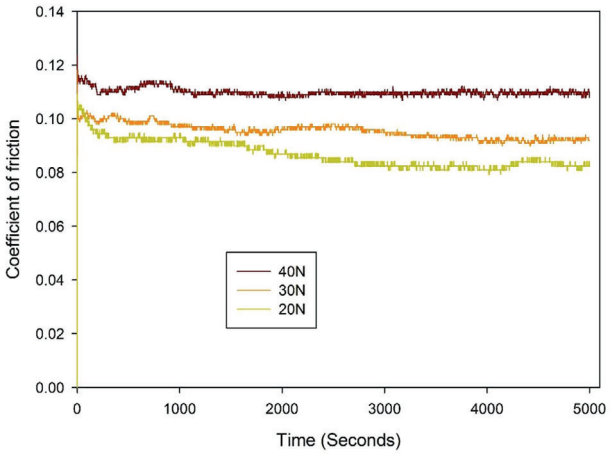

Figure 12. Coefficient of friction versus time at different normal loads, 5 Hz frequency at room temperature, with gear oil lubrication, tested in a 45° direction.

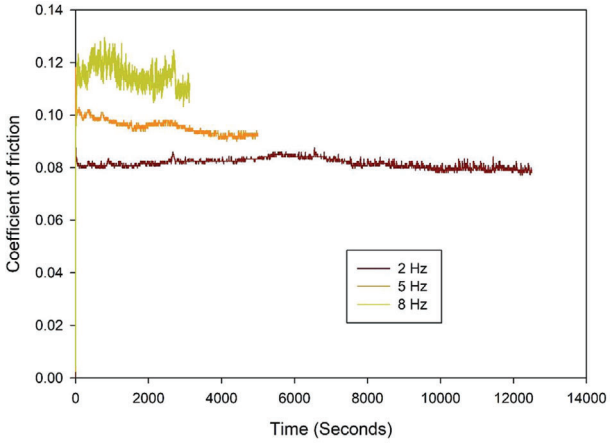

Figure 13. Coefficient of friction versus time at different frequencies, 30 N load at room temperature, with gear oil lubrication, tested in a 45° direction.

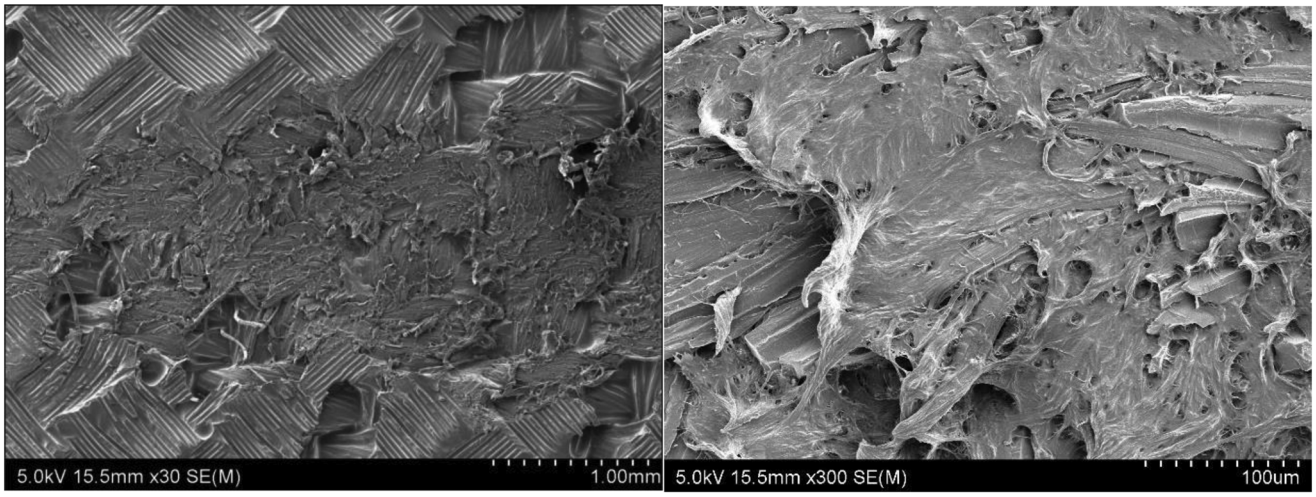

Figure 14. Wear track of the specimen tested under 30 N load, 5 Hz frequency at room temperature, with gear oil lubrication, in a 45° direction.

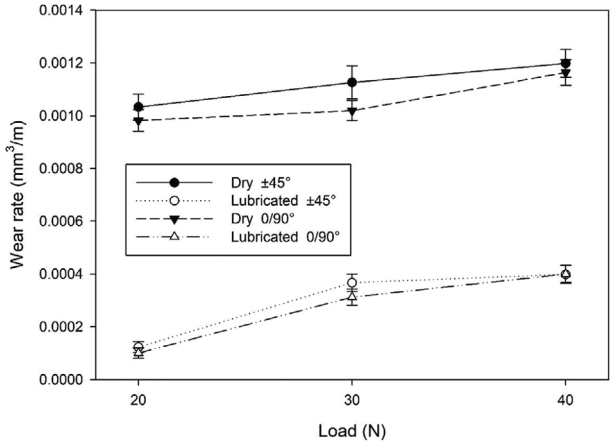

Figure 15. Wear rates at different normal loads, 5 Hz frequency and room temperature.

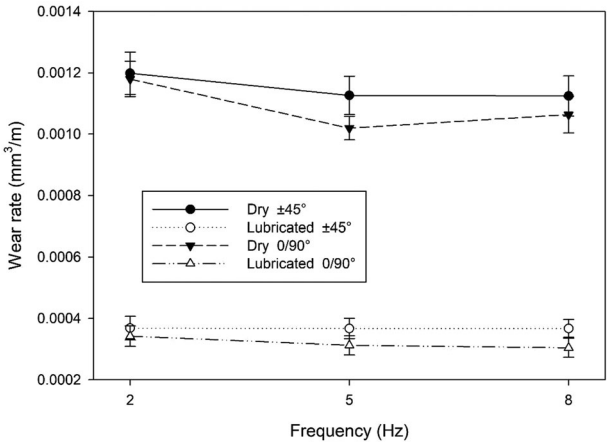

Figure 16. Wear rates at different frequencies, 30 N normal loads and room temperature.

increases. However, in all tested frequencies, COF remains at a low value below 0.12.

The SEM micrographs in **Figure 14** show that in the presence of a lubricant, the wear experienced by the composite material is significantly reduced. The lubricant serves to minimize friction and protect the material from direct contact, leading to a lower wear rate and minimal material removal. Some distortion of the epoxy polymer surrounding the bamboo fibers can be observed, along with tearing in certain areas. This suggests that, although the lubricant reduces the overall wear rate, some localized material deformation and damage still occur during the sliding process. However, the amount of wear observed under the lubricated contact condition is substantially lower than that experienced under dry contact conditions. This finding confirms the effectiveness of lubrication in improving the wear resistance and tribological properties of the bamboo composite material.

Wear rates at different normal loads are shown in **Figure 15**, for both dry and lubricated conditions. The results are presented for all three orientations of the bamboo fibers. As the composite material is made of a 0–90° woven textile (made from bamboo) embedded in an epoxy matrix, the mechanical and tribological properties in 0–90° directions are the same. It can be seen from Figure 15 that the wear rate is significantly lower in lubricated tests. In both dry and lubricated contact conditions, the wear rates in samples with 45° bamboo reinforcement direction are slightly higher than the 0–90° directions. This is because the force and sliding direction are not aligned with the woven threads in the 45° bamboo reinforcement direction, causing a shear deformation on the composite. The shear stresses induce the material's yielding, increasing the material loss and wear rate.

The effect of sliding speed (frequency) on wear rate is shown in **Figure 16**. Again, the composite material manufactured by 45° bamboo fabric orientation has a higher wear rate. In all sliding speeds, lubricated samples showed excellent wear resistance. Generally, as the frequency increases, the wear rate slightly decreases. This could be attributed to the reduction in contact time between the surfaces as sliding speed increases, leading to less accumulated wear over a given duration. The effect of test temperature on wear rate is presented in **Figure 17**. As the temperature increases, the wear rate increases, which is mainly due to

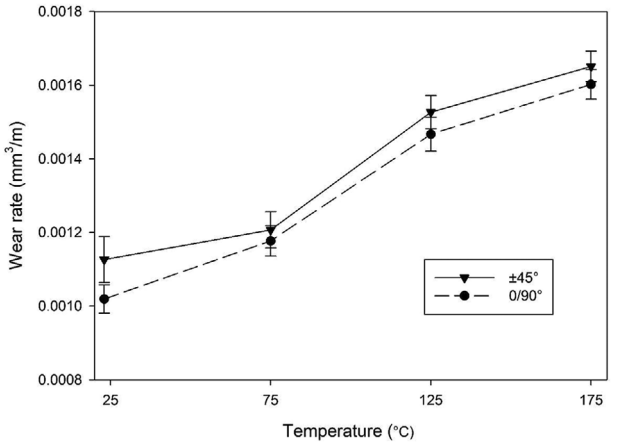

Figure 17. Wear rates at different temperatures, 30 N normal load and 5 Hz frequency.

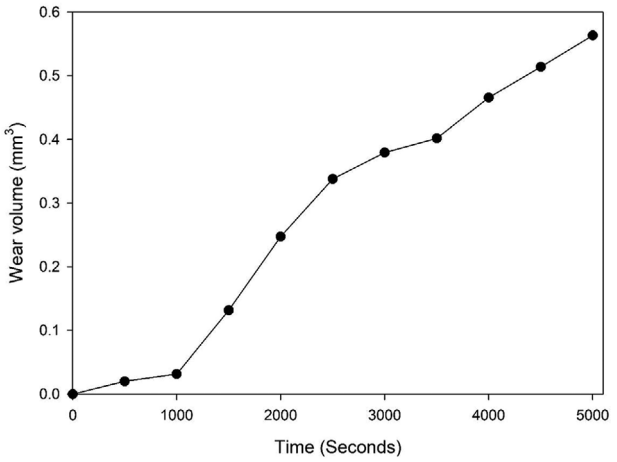

Figure 18. Wear rates versus time at room temperature, 30 N normal load and 5 Hz frequency under dry contact conditions.

the softening of the matrix at elevated temperatures. The softened matrix is more susceptible to deformation and material removal, resulting in an increased wear rate. However, the increase in wear volume is not remarkable, confirming that the developed composite material is suitable for high-temperature tribological applications. The material's ability to maintain its performance under elevated temperatures suggests potential use in various applications, such as automotive and aerospace components, where temperature-induced wear could be a significant concern.

To investigate the evolution of wear volume and wear rate during the tests, we stopped the tests at fixed intervals and measured the wear volumes, before putting the sample back into the tribometer and continuing the sliding wear test. **Figure 18** shows the wear volume measurements during a test conducted under 30 N normal load and 5 Hz frequency, at room temperature and dry contact. The results can be seen together in Figure 7. Up to ≈1000 s, the increase in wear volume is quite low, corresponding to the low COF in Figure 6. The wear rate increases significantly as the COF increases after this time. After 1000 s, the increase in wear volume is higher for the remainder of the test. Figure 18 shows that the change in wear volume is gradual and almost linear during the sliding wear test, indicating the good bond between the bamboo fabric and the epoxy matrix layers. This strong interfacial adhesion contributes to the material's consistent wear behavior and overall durability, making it a promising candidate for various tribological applications.

4. Conclusion

This paper presented a detailed experimental approach to characterize the tribological performance of the developed bamboo fabric-reinforced epoxy composite. The effects of working conditions, that is, applied load, sliding frequency, lubrication and temperature on wear rate, coefficient of friction, and wear mechanisms of the composite material were investigated. Higher wear rates were observed at higher applied loads and temperatures. Under lubricated contact conditions, the composite material showed a low coefficient of friction and very good wear resistance.

The COF curves in dry contact generally showed three stages of wear. In the first stage, a low COF was observed until the top matrix layer wears out and the counter ball is in direct contact with the bamboo fabric. In the second stage, we observed a jump in friction coefficient and the contact stress between the ball and the bamboo fabric causes excessive wear and the release of bamboo fiber and epoxy resin wear debris in the contact interface. This debris further accelerates the wear loss and at the third stage, we could see the friction coefficients reach a stable level, albeit with significant fluctuations. At this final stage, the debris completely covered the wear scars and grooves of the wear track. Different stages' duration and starting time depend on the sliding wear conditions, that is, average load, frequency, and specimen temperature.

Based on SEM observations, generally under nonlubricated conditions, the sliding wear caused the fabric distortion and eventually destroyed the layers of fibers. The damage to the reinforcement phase accelerated the wear deterioration. For lubricated conditions, the lubricant thin film was effective and reduced the friction coefficient and protected the top resin layer from being completely worn off, therefore, very low wear rates were recorded for lubricated tests.

Based on the results, the composite materials produced by 0–90° bamboo fabric orientations had slightly better wear resistance. This was attributed to the extra shear stress experienced by the fabric in a 45° orientation. The composite materials made by 0° and 90° bamboo fabric orientations showed the same level of wear volume and friction coefficient. Abrasive wear and fatigue wear were the main wear mechanisms for the developed composite material tested at room temperature, while adhesive wear was also detected in the samples tested at elevated temperatures.

Acknowledgements

This research is a part of the grant "Investigación aplicada para el desarrollo de materiales compuestos de alta sostenibilidad (INNEST/2022/272)" funded by the Agència Valencia de la Innovació-AVI. Funding for open access charge: CRUE- Universitat Politècnica de València.

Conflict of Interest

The authors declare no conflict of interest.

Data Availability Statement

The data that support the findings of this study are available from the corresponding author upon reasonable request.

Keywords

composite materials, tribology, wear resistance, woven bamboo fabrics

Received: March 7, 2023
Revised: May 9, 2023
Published online:

[1] T. Sathish, P. Jagadeesh, S. M. Rangappa, S. Siengchin, *Pol. Comp.* **2022**, *43*, 4700.
[2] B. K. Venkatesha, S. K. Pramod Kumar, R. Saravanan, A. Ishak, *IOP Conf.: Mater. Sci. and Eng.* **2020**, *1003*, 012087.
[3] N. Z. M. Zuhudi, K. Jayaraman, R. J. T. Lin, N. M. Nur, *IOP Conf.: Mater. Sci. and Eng.* **2018**, *370*, 012047.
[4] P. Kandhavadivu, M. Parthiban, *Indian J. of Fib. Tex. Res.* **2022**, *47*, 64917.
[5] X. Pei, Q. Jiang, J. Lin, T. Li, L. Wu, H. Peng, *Mater. Rep.* **2017**, *31*, 55.
[6] N. Z. M. Zuhudi, K. Jayaraman, R. J. T. Lin, *Pol. and Pol. Comp.* **2016**, *24*, 755.
[7] N. Kumari, K. Kumar, *Mater. Today Proc.* **2021**, *46*, 243.
[8] K. Yorseng, S. Mavinkere, J. Parameswaranpillai, S. Siengchin, *J. Clean Prod.* **2022**, *363*, 132314.
[9] K. V. Chalapathi, J. I. Song, M. N. Prabhakar, *J. Nat. Fib.* **2022**, *19*, 2129.
[10] H. A. Kim, *J. Tex. Inst.* **2021**, *112*, 1940.
[11] M. R. Fazita, K. Jayaraman, D. Bhattacharyya, M. S. Hossain, M. K. Haafiz, A. H. P. S. Abdul, *Polymers* **2015**, *7*, 1476.
[12] C. W. Chin, B. F. Yousif, *Wear* **2009**, *267*, 1550.
[13] L. A. Pothan, J. George, S. Thomas, *Comp. Interf.* **2002**, *9*, 335.
[14] M. A. Maleque, F. Belal, S. M. Sapuan, *Arab. J. Sci. and Eng.* **2007**, *32*, 359.
[15] M. Jacob, S. Thomas, K. T. Varughese, *J. Appl. Pol. Sci.* **2004**, *93*, 2305.
[16] B. F. Yousif, N. S. M. El-Tayeb, *Surf. Rev. and Lett.* **2007**, *14*, 1095.
[17] N. S. El-Tayeb, *Wear* **2008**, *265*, 223.
[18] U. Nirmal, B. F. Yousif, D. Rilling, P. Brevern, *Wear* **2010**, *268*, 1354.
[19] Y. Dessalegn, B. Singh, A. W. Van Vuure, A. A. Rajhi, G. M. S. Ahmed, N. Hossain, *Materials* **2022**, *15*, 4144.
[20] B. Oliver-Borrachero, S. Sanchez-Caballero, O. Fenollar, M. A. Selles, *Key Eng. Mater.* **2019**, *793*, 9.
[21] J. F. Scherer, R. P. Bom, R. Barbieri, *Eng. Res. Exp.* **2020**, *2*, 015018.
[22] A. Porras, A. Maranon, *Comp. Part B: Eng.* **2012**, *43*, 2782.
[23] C. Zhao, G. Song, H. Liu, *Adv. Mater. Res.* **2011**, *331*, 89.
[24] B. Rashid, M. Jawaid, H. Fouad, N. Saba, S. Awad, E. Khalaf, M. Sain, *Pol. Comp.* **2022**, *43*, 3167.
[25] M. Montiel, "Cultivo y uso del bambú en el neotrópico", https://www.anc.cr/publicaciones/Revista-Biolog%C3%ADa-Tropical/Volumen_46/Cultivo-y-uso-del-Bamb%C3%BA-en-el-Neotr%C3%B3pical/11-Montiel--El-bamb%C3%BA-revisi%C3%B3n-de-su-biolog%C3%ADa-y-cultivo/, accessed: April, **2023**.
[26] N. Kaur, S. Saxena, H. Gaur, P. Goyal, in *Int. Conf. Inf. Tech. and Un. Sys.*, IEEE, New York City, NY, USA **2017**, pp. 843–849.
[27] M. Das, in *Composite Materials*, Springer, Berlin, Heidelberg, Germany **2017**.
[28] N. Sukumar, M. Bayeleyegn, S. Aruna, *Res. J. Tex. App.* **2022**, *26*, 73.
[29] S. N. Sarmin, M. Jawaid, M. H. Mahmoud, N. Saba, H. Fouad, O. Y. Alothman, C. Santulli, *Bio. Conv. Bioref.* **2022**, https://doi.org/10.1007/s13399-022-02872-9.
[30] S. Salim, T. Rihayat, S. Riskina, A. Safitri, *Plast. Rub. Comp.* **2021**, *50*, 415.
[31] V. V. Raman, P. S. Kumar, P. Sunagar, K. Bommanna, R. Vezhavendhan, R. S. Bhattacharya, S. V. Prabhu, B. Sasikumar, *Adv. Pol. Tech.* **2022**, *2022*, 9133411.
[32] H. Khazal, S. Abbas, Y. Younis, M. Rahman, T. Jamil, T. Jamil, *Eur. J. Appl. Eng. Sci. Res.* **2021**, *19*, 119.
[33] B. K. Venkatesh, R. Saravanan, *Int. J. Veh. Struct. Sys.* **2020**, *12*, 447.
[34] T. Richmond, L. Lods, J. Dandurand, E. Dantras, C. Lacabanne, S. Malburet, A. Graillot, J. M. Durand, E. Sherwood, P. Ponteins, *Mater. Res. Exp.* **2022**, *9*, 015505.
[35] S. Zhou, J. Li, S. Kang, D. Zhang, *J. Nat. Fib.* **2022**, *19*, 1239.
[36] A. B. M. Supian, M. Jawaid, B. Rashid, H. Fouad, N. Saba, H. N. Dhakal, R. Khiari, *J. Mater. Res. Tech.* **2021**, *15*, 1330.
[37] J. D. D. James, R. Mohan, R. Vijay, *Mater. Today: Proc.* **2020**, *39*, 1.
[38] A. Eid Alajmi, J. G. H. Alotaibi, B. F. Yousif, U. Nirmal, *Polymers* **2021**, *13*, 2444.
[39] R. Shi, X. Sheng, H. Jia, J. Zhang, N. Li, H. Shi, M. Niu, Q. Ping, *Mater. Eng.* **2022**, *307*, 2100745.
[40] F. Wang, J. Shao, X. Li, *Polym. Compos.* **2016**, *37*, 221.
[41] F. Wang, M. Yang, S. Zhou, S. Ran, J. Zhang, *J. Appl. Polym. Sci.* **2017**, *135*, 46148.
[42] 1050 epoxi resin, www.resoltech.com/en/, accessed: April, **2023**.

